A peer-reviewed version of this preprint was published in PeerJ on 18 November 2014.

Wilson PG, Payne T. 2014. Genetic reprogramming of human amniotic cells with episomal vectors: neural rosettes as sentinels in candidate selection for validation assays. PeerJ 2:e668
https://doi.org/10.7717/peerj.668

Genetic reprogramming of human amniotic cells with episomal vectors: Neural rosettes as sentinels in candidate selection for validation assays

The promise of genetic reprogramming has prompted initiatives to develop banks of induced pluripotent stem cells (iPSCs) from diverse sources. Sentinel assays for pluripotency could maximize available resources for generating iPSCs. Neural rosettes represent a primitive neural tissue that is unique to differentiating PSCs and commonly used to identify derivative neural/stem progenitors. Here, neural rosettes were used as a sentinel assay for pluripotency in selection of candidates to advance to validation assays. Candidate iPSCs were generated from independent populations of amniotic cells with episomal vectors. Phase imaging of living back up cultures showed neural rosettes in 2 of the 5 candidate populations. Rosettes were immunopositive for the Sox1, Sox2, Pax6 and Pax7 transcription factors that govern neural development in the earliest stage of development and for the Isl1/2 and Otx2 transcription factors that are expressed in the dorsal and ventral domains, respectively, of the neural tube in vivo. Dissociation of rosettes produced cultures of differentiation competent neural/stem progenitors that generated immature neurons that were immunopositive for Beta III-tubulin and glia that were immunopositive for GFAP. Subsequent validation assays of selected candidates showed induced expression of endogenous pluripotency genes, epigenetic modification of chromatin and formation of teratomas in immunodeficient mice that contained derivatives of the 3 embryonic germ layers. Validated lines were vector-free and maintained a normal karyotype for more than 60 passages. The credibility of rosette assembly as a sentinel assay for PSCs is supported by coordinate loss of nuclear-localized pluripotency factors Oct4 and Nanog in neural rosettes that emerge spontaneously in cultures of self-renewing validated lines. Taken together, these findings demonstrate value in neural rosettes as

PeerJ PrePrints | http://dx.doi.org/10.7287/peerj.preprints.449v1 | CC-BY 4.0 Open Access | received: 31 Jul 2014, published: 31 Jul

sentinels for pluripotency and selection of promising candidates for advance to validation assays.

PeerJ PrePrints | http://dx.doi.org/10.7287/peerj.preprints.449v1 | CC-BY 4.0 Open Access | received: 31 Jul 2014, published: 31 Jul

Genetic reprogramming of human amniotic cells with episomal vectors: Neural rosettes as sentinels in candidate selection for validation assays

Patricia G. Wilson, Ph. D.[1,3] and Tiffany Payne[2]

[1] Institute for Regenerative Medicine, Wake Forest School of Medicine, Medical Center Blvd., Winston Salem NC 27157

[2] Wake Forest University, 1834 Wake Forest Rd, Winston-Salem, NC 27106

[3]Corresponding author: Dr. Patricia G. Wilson

Institute for Regenerative Medicine

Wake Forest School of Medicine

Medical Center Blvd.

Winston Salem NC 207157

Tele: 336.713.7297

email: pgwilson@wakehealth.edu,

Author contact information

PeerJ PrePrints | http://dx.doi.org/10.7287/peerj.preprints.449v1 | CC-BY 4.0 Open Access | received: 31 Jul 2014, published: 31 Jul

16 Patricia G. Wilson, Ph. D.
17 Institute for Regenerative Medicine
18 Medical Center Blvd.
19 Winston Salem NC 27157
20 336-713-7297
21 pgwilson@wakehealth.edu

22 Tiffany Payne
23 tmpayne0409@email.campbell.edu
24 336-240-5796
25 515 Deaton Young Rd
26 Lexington, NC 27292

Abstract

The promise of genetic reprogramming has prompted initiatives to develop banks of induced pluripotent stem cells (iPSCs) from diverse sources. Sentinel assays for pluripotency could maximize available resources for generating iPSCs. Neural rosettes represent a primitive neural tissue that is unique to differentiating PSCs and commonly used to identify derivative neural/stem progenitors. Here, neural rosettes were used as a sentinel assay for pluripotency in selection of candidates to advance to validation assays. Candidate iPSCs were generated from independent populations of amniotic cells with episomal vectors. Phase imaging of living back up cultures showed neural rosettes in 2 of the 5 candidate populations. Rosettes were immunopositive for the Sox1, Sox2, Pax6 and Pax7 transcription factors that govern neural development in the earliest stage of development and for the Isl1/2 and Otx2 transcription factors that are expressed in the dorsal and ventral domains, respectively, of the neural tube in vivo. Dissociation of rosettes produced cultures of differentiation competent neural/stem progenitors that generated immature neurons that were immunopositive for βIII-tubulin and glia that were immunopositive for GFAP. Subsequent validation assays of selected candidates showed induced expression of endogenous pluripotency genes, epigenetic modification of chromatin and formation of teratomas in immunodeficient mice that contained derivatives of the 3 embryonic germ layers. Validated lines were vector-free and maintained a normal karyotype for more than 60 passages. The credibility of rosette assembly as a sentinel assay for PSCs is supported by coordinate loss of nuclear-localized pluripotency factors Oct4 and Nanog in neural rosettes that emerge spontaneously in cultures of self-renewing validated lines. Taken together, these findings demonstrate value in neural rosettes as sentinels for pluripotency and selection of promising candidates for advance to validation assays.

Key words: genetic reprogramming, neural rosettes, episome, amniotic

Introduction

Genetic reprogramming offers unprecedented opportunities for regenerative medicine (Robinton & Daley 2012; Trounson et al. 2012; Yamanaka 2012). Genetic reprogramming of fetal cells in amniocentesis samples (Ferguson-Smith 2008) is a feasible path to fetus-specific iPSCs for testing the efficacy of pharmaceuticals and for postnatal therapies. From a practical viewpoint, reprogramming of autologous fetal cells for translational use is less likely in the foreseeable future than use of immunologically compatible iPSCs from allogenic sources that have been reprogrammed and manufactured with GMP compliant standards (Turner et al. 2013). From this standpoint, fetal cells in amniotic fluid are attractive because they are among the youngest cells available with minimally invasive procedures.

Amniotic cells are unique among targets for genetic reprogramming in that they are drawn from a fluid-filled reservoir rather than a vascularized tissue. Amniocentesis samples contain a mixture of cells that are sloughed from exposed fetal and placental surfaces into amniotic fluid (Maguire et al. 2013; Wilson et al. 2012). Although amniotic cells are most widely known as stromal cells (Murphy & Atala 2013), fetal skin and placental membranes expose the largest surface area to amniotic fluid (Dobreva et al. 2010) and these epithelia are likely significant contributors of cells to amniocentesis samples (Jezierski et al. 2010). Amniotic fluid is primarily derived by flow from the placenta and fetal lungs into the amniotic sac (Brace 1997) and it is composed mainly of water with some electrolytes and urea from fetal urine (Underwood et al. 2005). A small subset of cells in amniocentesis samples can proliferate in serum-containing media ex vivo; clonal analysis of independent amniocentesis samples indicate that the vast majority of cells do not proliferate and that cultures are established by fewer than 15 founder amniotic cells (Wilson et al. 2012). Amniotic cell cultures show diversity within and among cell populations (Wilson et al. 2012) that may reflect genetic differences and sampling as well as congenital influences such as placental function, environmental toxins, maternal hormones or simply the length of time that founder cells remained in amniotic fluid before ex vivo culture. The impact of the gestational environment on amniotic cells is not well established and likely to vary among cells, but it is clear that these cells have a finite lifespan in culture and eventually undergo senescence (Wolfrum et al. 2010).

Genetic reprogramming can be incomplete and costly in time and resources as a result. Methods to quickly identify promising candidates can reduce this investment and differentiation potential

is a logical metric. Neural differentiation of PSCs has been well characterized and is manifest in living cultures by assembly of neural rosettes (Elkabetz et al. 2008; Liu & Zhang 2011; Wilson & Stice 2006; Zhang 2006), radial arrangements of polarized neuroepithelial stem cells, designated here as neural stem/progenitors (NSPs). Rosette assembly and differentiation recapitulates well characterized pathways of neurodevelopment in vivo (Cohen et al. 2013). The transition of PSCs through specification of neuroepithelial stem cells and restriction of cell fate to region-specific subtypes can be traced by spatial and temporal expression of transcription factors that govern neural development in vivo (Elkabetz & Studer 2008; Wilson & Stice 2006). Rosette assembly has primarily been used primarily to characterize neural differentiation in established PSC lines (Elkabetz & Studer 2008; Shin et al. 2006), but it is widely recognized and recently documented that neural rosettes emerge spontaneously in cultures of self-renewing PSCs as (Malchenko et al. 2014).

Amniotic cells have been reprogrammed with viral vectors, including both integrating (Anchan et al. 2011; Fan et al. 2012; Galende et al. 2010; Ge et al. 2012; Li et al. 2009; Li et al. 2012; Liu et al. 2012; Lu et al. 2011; Wolfrum et al. 2010; Ye et al. 2010) and nonintegrating systems (Jiang et al. 2014), that efficiently deliver reprogramming transgenes. Leaky or reactivated expression of integrated vector transgenes can hinder differentiation and induce tumors in vivo (Malik & Rao 2013; Mostoslavsky 2012; Rao & Malik 2012), blocking clinical translation as a result. Nonintegrating vectors circumvent this barrier (Mostoslavsky 2012) and transgene-free iPSCs have been derived from stromal cells in amniotic fluid using a commercial source of nonintegrating Sendai viral vectors (Jiang et al. 2014).

Nonintegrating episomal vectors for reprogramming are attractive because they are easily accessible and cheaply amplified with well-established methods that are used in most research labs (Mostoslavsky 2012). Vectors have improved since their introduction, but reprogramming efficiency of episomal systems remains lower than that of viral systems. Here we report use of first-generation episomal vectors (Yu et al. 2009) to genetically reprogram independent amniotic cell populations that we established in a previous work (Wilson et al. 2012). Our strategy was to use assembly of neural rosettes as a sentinel assay to screen and select candidates to advance for validation assays.

Materials and Methods

Amniotic cell sources and nomenclature

Amniotic cell populations were derived from amniocentesis samples (Wilson et al. 2012) that were donated with informed consent and a protocol approved by the Institutional Review Board of Wake Forest University Health Sciences (IRB#00007486). We were blinded to age of the mother, period of gestation or the results of diagnostic tests. Amniotic cell lines were assigned an identifier for the Christopher Moseley (ChM) Foundation as the funding source and a unique identifier: each mixed cell population was assigned a number each clonal line was assigned a alphanumeric identifier to reflect the amniocentesis sample and the specific clonal line (Wilson et al. 2012). For example, the ChM5 and ChM1 populations were isolated as mixed cell populations and the ChMRCB1 population was isolated as a clonal population by limiting dilution of the RC amniocentesis sample that produced this clone in the B1 well of a 12 well plate (Wilson et al. 2012). Following transfection of target cells and colony isolation, derivative lines were indicated as iChM5 or iChMRCB1 candidates or validated iPSCs. By convention the passages (p) number is indicated as an extension of the population name where relevant. iChM5A and iChM5B are referred to collective as iChM5 derivatives for simplicity and likewise, independent candidate lines that were derived from ChMRCB1 cells are referred to as independent iChMRCB1 derivatives.

Somatic cell culture

Amniotic cells and HEK293 cells were maintained in DMEM15% (DMEM supplemented to 15% fetal bovine serum (FBS), 1% L-glutamine and 1% penicillin/streptomycin solution). Cells were routinely maintained on culture wares pretreated with 1:100 dilution of growth factor reduced matrigel (BD Biosciences). All media components in this work were obtained from Life Technologies unless stated otherwise.

PSC cell culture

The H9 (WA09) line of human embryonic stem cells (hESCs) and iPSC lines were maintained and/or established with a feeder-dependent culture system and standard hESC media supplemented with 1% penicillin/streptomycin solution on mitomycin-C inactivated mouse embryonic fibroblasts (MEFs) as recommended by the National Stem Cell Bank (NSCB, Madison WI). MEFs were generated from 13-day old CF-1 embryos (Charles River, Inc) and

following expansion and mitomycin-C treatment, MEFs were washed extensively with Dulbecco's phosphate buffered saline (DPBS; Life Technologies), harvested with Accutase (Life Technologies) and replated in MEF media on culture wares near 2 x 10^5 cells/cm^2 for immediate use or cryropreserved with standard methods after 24 hr recovery. Conditioned hESC media was prepared by culture of inactivated MEFs in hESC media without bFGF for 24 hrs, supplemented with 4 ng/ml bFGF and filtered sterilized before use. Feeder-free cultures were maintained in MEF-conditioned hESC media, mTeSR-1 (StemCell Technologies) or Essential 8 (Life Technologies) media. Passaging of PSCs cultured on MEF feeders or in MEF-conditioned media was done by manual microdissection of optimal undifferentiated colonies with a fire-polished glass pipette using a dissecting microscope. Feeder-free cultures were passaged with EDTA as described (Beers et al. 2012). The ROCK inhibitor Y27632 (Tocris) was routinely added at 5 µM/ml media for 24 h post-passage.

Genetic reprogramming

The episomal vectors (Addgene, Inc.) that were used in this work are described in Supplementary Table 1. Episomal vectors were amplified in Top10 bacteria with antibiotic selection in standard Luria Broth and extracted with DNAeasy Kits (Qiagen, Inc) with good recovery of DNA. In each experiment ~ 8 x 10^5 target cells were seeded at subconfluent densities ~ 1.4 x 10^3 cells/cm^2 and transfected the following day with pooled plasmid combinations in equimolar ratios (~ 0.2 µg DNA /cm^2) with Fugene HD (Promega, Corp.) 0.15 µl /µg DNA at 8 to 12 hr intervals for a total of 3 transfections. Transfected cells were maintained in DMEM15% for ~ 4 days and then switched to MEF conditioned hESC media supplemented with 2.5 mM valproic acid (Sigma-Aldrich) for ~ 2 weeks after colonies appeared. Independent populations of ChMRCB1p3 cells were transfected with the 3-vector combination and 7 to 9 colonies were recovered from each population. A single representative colony was selected from each and maintained separately as iChMRCB1.A, iChMRCB1.C, and iChMRCB1.E candidate populations. A population of ChM5p10 cells was transfected with the 2-vector combination, but the population became highly confluent in hESC media within 2 weeks and potential colonies were difficult to identify. The transfected population was passaged with Accutase and replated on MEF feeders. hESC-like colonies emerged within 2 weeks, optimal colonies were pooled and maintained as the iChM5A candidate population. Transfected ChM5p12 cells were maintained for 4 days in growth media, treated with Accutase and passaged to MEF feeders as separate populations; a single hESC-like

colony was recovered from one population of transfected cells and maintained as the iChM5B candidate population. Optimal hESC-like candidate colonies and control H9 hESC colonies were passaged as needed to maintain healthy cultures.

Neural differentiation

Following the first manual passage of candidate colonies from MEF feeders, residual colony fragments in the primary culture plate were maintained in conditioned hESC media for 3 to 5 days to allow colony expansion and then switched to regular hESC media to encourage spontaneous differentiation as the MEF feeders age and pluripotency of the expanding population by bFGF in hESC media. Rosettes were manually isolated as they emerged and passaged in hESC media to matrigel-treated cover slips for immunostaining. Long term cultures of neural progenitors/stem cells (NSPs) were established as described (Shin et al. 2006); neural rosettes were serially passaged for 2 or 3 times to enrich for rosettes before dissociation with Accutase and population expansion. Rosette-derived NSP cultures and a commercial source (Millipore) immortalized human midbrain NSPs (hVMNSPs) were maintained in ReNcell NSC Maintenance Media (Millipore) supplemented with 20 ng/ml bFGF and 20 ng/ml EGF or a proliferation media (1:1 mix of DMEM/F-12 and Neurobasal media, 1% L-glutamine and 1% penicillin/streptomycin solution, 0.5 X B27, 0.5X N2, 20 ng/ml bFGF and 20 ng/ml EGF) as described (Brace 1997). Differentiation of NSPs was induced by withdrawal of bFGF and EFG from proliferation media. Rosette collections and NSPs were cryropreserved in proliferation media supplemented with 10% DMSO with standard methods. Addition of ROCK inhibitor greatly improved survival at thaw.

PCR detection of transgene and vector sequences

Total cellular DNA was isolated with GenePure (Qiagen) or QiaAmp DNA Mini (Qiagen) kits and treated with RNAse to remove RNA. Transgenes or endogenous genes were amplified in reactions containing 100 ng genomic DNA or < 1ng plasmid DNA with GC-rich polymerase (Life Technologies) in 1X Buffer A, 3 µl of Enhancer and 250nM of oligonucleotide primers (Supplementary Table 2) with touchdown cycling conditions: 1 cycle [95 ºC for 10min], 2 cycles [95 ºC for 1 min, 64 ºC for 1 min, 72 ºC for 1 min], 2 cycles [95ºC for 1 min, 62 ºC for 1 min, 72ºC for 1 min], 2 cycles [95 ºC for 1 min, 60 ºC for 1 min, 72 ºC for 1 min], 35 cycles [95ºC for 1 min, 58 ºC for 1 min, 72 ºC for 1 min] and 1 cycle [72 ºC 10 min].

Transcript analysis

Total cellular RNA was isolated with RNAeasy kits (Qiagen) and contaminating DNA was removed by DNAse treatment. RNA was converted to cDNA using SuperScript First-Strand Synthesis System (Life Technologies) and 1 µl of 1:4 dilution of cDNA in water was amplified in each reaction. Transcript levels in Fig. 4D were assayed with QuantiTect Syber Green primer assays (Qiagen) with the exception of cMyc (Supplementary Table 2) with FastStart Universal SYBR Green Master Mix (Roche/Life Technologies). Transcript levels in Fig. 4E were established with TaqMan assays with TaqMan® Gene Expression Master Mix (Life Technologies).

Bisulfite sequencing

Genomic DNA was processed with an Epitect kit (Qiagen) as directed by vendor. Amplification products were generated with primers that were specific to converted DNA (Supplementary Table 2), purified with a Qiaquick PCR purification kit and cloned with a TOPO-TA PCR4 cloning kit (Life Technologies). Plasmid DNA was purified with QIAprep Spin Miniprep kits (Qiagen) or EconoSpin columns (Epoch) and sequenced directly or the vector inserts were first amplified with M13 primers using High Fidelity EcoDry PCR mix (Promega, Corp.) as follows: 95ºC for 10 min, 40 cycles (95ºC for 15 sec, 54ºCfor 30 sec and 68ºC for 30 sec), 68ºC for 10 min. Amplification products were column-purified and sequenced directly (Operon or Genewiz). Data was imported into the SeaView graphical software program for alignment and analysis.

Imaging and immunocytochemistry

Cells were cultured in multiwell tissue culture plates on cover glass or in multiwall chamber slides that were pretreated with 1:100 dilution of growth factor reduced matrigel. Samples were fixed and immunostained as described (Wilson et al. 2012) with antibodies tabulated in Supplementary Table 3. Wide-field images were captured with ImagePro software using a QImaging CCD camera mounted on a Leica upright microscope. Immunostaining was repeated in at least 2 technical replicates and in more than 3 independent trials for each marker/combination tested. The images shown throughout this manuscript are representative; our conclusions were based on at least 3 fields of view for each replicate and inspection of more than 500 cells for detection of each antigen. Virtually all experiments were done in parallel with positive and negative controls, typically H9 hESCs, parental ChM5 cells or HEK293 as appropriate for the antigen.

Results

Target amniotic cell populations and episomal vectors

Reprogramming targets were selected from a collection of mixed cell pools and clonal lines of amniotic cells that were isolated from independent amniocentesis samples by minimal and limiting dilution, respectively, in serum-containing media (Wilson et al. 2012). Nomenclature and conventions for indicating passage number for amniotic cell populations are described in Experimental Procedures. Targets were selected to reflect the range of cell types in amniocentesis samples and proliferation characteristics that we considered to be important to the efficiency of reprogramming. The ChM5 mixed cell population was highly enriched for fibroblast-like stromal cells and cell proliferation continues in confluent cultures. The ChMRCB1 clonal population of epithelial cells continues to expand in subconfluent cultures, but shows contact inhibition of proliferation in confluent cultures (Wilson et al. 2012), verified by the absence of mitotic figures by immunofluorescence analysis of chromosomes and spindle microtubules (data not shown). The H9 (Thomson et al. 1998) line of human embryonic stem cells (hESCs) provided a positive control throughout.

Reprogramming used combinations of 2 or 3 first generation episomal vectors (Supplementary Table 1) that collectively encoded the four Yamanaka factors Oct4, Sox2, Klf4, cMyc (Takahashi et al. 2007) as well as Nanog, Lin28 and the Large T antigen of SV40 (Yu et al. 2009). Preliminary experiments showed efficient transfection of HEK293 cells with Fugene-HD and correlated maintenance of vector sequences with immunostaining of Oct4 (Supplementary Fig.1). The efficiency of chemical transfection of amniotic cell targets was low; less than 5% were immunopositive for Oct4 at 48 hrs post-transfection. Subconfluent cultures of ~ $8x10^5$ cells were serially transfected every 8 to 12 hours for 3 transfections in order to increase the number of transfected cells.

Recovery and preliminary screen of candidate iPSC colonies

Candidate colonies were recovered from all of amniotic cell populations that we tested. ChMRCB1p6 cells were transfected with the 3-vector combination in 3 separate populations and 7 to 9 candidate colonies were generated in each population. A representative colony was isolated from each population and the iChMRCB1.A, iChMRCB1.C, and iChMRCB1.E derivatives were

expanded independently. ChM5p10 and ChM5p12 cells were transfected with the 2- and 3-vector combination, respectively (Supplementary Table 1) and optimal colonies were pooled and designated as iChM5A and iChM5B, respectively. Colonies of iChM5 derivatives were compact with well defined edges, but colonies in iChMRCB1 derivatives were less compact. Cells in candidate colonies were small (~15 µm in diameter) in comparison to the size of parental amniotic cells (~50 µm to 150 µm in diameter), primarily due to apparent reduction in the amount of cytoplasm (Fig. 1). Immunostaining showed Oct4 expression that was similar to H9 hESCs, but included a subset of cells that showed obviously higher levels of Oct4 expression (Fig. 1) that may reflect induced expression of the endogenous Oct4 gene superimposed with transgene expression. Neither parental ChM5 nor ChMRCB1 cells ($n \geq 500$ in 3 experiments) showed nuclear localized Oct4 by immunofluorescence using the same monoclonal antibody (data not shown). Taken together, these observations suggested that candidate colonies did not reflect preexisting Oct4-expressing cells. The frequencies of candidate colonies, 1 to 10 independent candidates from ~8 x 10^5 transfected cells, was similar to previous studies using these vectors (Yu et al. 2009). Given the low efficiency of chemical transfection, the actual rate may have been higher.

Self-assembly and differentiation of neural rosettes in candidate populations

Optimal colonies were manually passaged by microdissection and sibling colony fragments were maintained in the original plate as back up cultures and screened for evidence of differentiation. Backup cultures were initially maintained in conditioned hESC media for 3 to 5 days to ensure survival of the new culture and then switched to hESC to encourage spontaneous differentiation as feeder layers age. Rosettes did not appear in any of the backup cultures of the 3 independent lines of iChMRCB1 candidates, despite expansion in serial passages. Neural rosettes emerged within ~ 2 weeks in back up cultures of iChM5A and iChM5B candidates that were indistinguishable from rosettes in control H9 hESCs (Fig. 2, Supplementary Fig. 2). Rosettes were manually isolated by microdissection as they emerged in sequential backup cultures of iChM5A (p3 and p4) and iChM5B (p4 and p6) and transferred to hESC media on matrigel coated substrates for immunofluorescence analysis or to a proliferation media for cryopreservation. Immunostaining showed nuclear localization of the Sox1, Sox2, Pax6, Pax7transcription factors (Fig. 2, Supplementary Fig. 2) that regulate specification of neuroectoderm in vivo and the Otx2 and Isl1/2 transcription factors that determine neural subtype identity in the dorsal and ventral

domains, respectively, of the neural tube (Elkabetz & Studer 2008; Hitoshi et al. 2004; Liu & Zhang 2011; Wilson & Stice 2006; Zhang 2006). Immunodetection of this collection of transcription factors provided strong evidence that the isolated structures were neural rosettes and while rosette collections were immunopositive for the intermediate filament proteins nestin and vimentin (Supplementary Fig. 2) that are commonly used as cytoplasmic markers of neural identity, but these proteins not exclusive to neural derivatives. All of the rosette collections that we tested showed apparent immature neurons with long axonal-like projections that were immunopositive for βIII-tubulin (Fig. 2, Supplementary Fig. 2). Because rosettes are unique to PSCs, we interpreted these findings as preliminary evidence for pluripotency of iChM5 candidates. Given the absence of rosettes, iChMRCB1 candidates were not pursued further here.

Neural rosettes derived from established lines of hESCs and iPSCs are a source of proliferating NSP cultures (Elkabetz & Studer 2008; Shin et al. 2006). To test whether NSPs could be derived from iChM5 candidates, iChM5A and iChM5B candidates were differentiated toward neural lineages with an established protocol (Shin et al. 2006). Rosettes were manually isolated and enriched by serially passage in a proliferation media and then dissociated to generate monolayer cultures of proliferating NSPs. NSP cultures were generated from both candidates, but we focused on the NSP population that was isolated from iChM5B cultures at passage 6 (NSPB6); this population showed more than 95% of NSPs were immunopositive for Sox1, a few βIII-tubulin immunopositive immature neurons (Fig. 2). A portion of the NSPB6 population shown in Fig. 2 was maintained in culture for more than 30 passages and produced dense mats of immature neurons that were immunopositive for βIII-tubulin (Fig. 2; Supplementary Fig. 3) when differentiation was induced by withdrawal of mitogens from proliferation media. Apparent glia, cells immunopositive for glia fibrillary acidic protein (GFAP), were infrequent (<1%) in all NSP populations, likely reflecting the known delay of gliogenesis relative to neurogenesis (Wilson & Stice 2006). Although our analysis was not exhaustive, these findings showed derivation of differentiation-competent NSPs and provide added support for pluripotency of iChM5 derivatives and advance to validation assays.

Validation of self-renewing, karyotypically normal and pluripotent iChM5 lines

Pluripotency of iChM5 derivatives was tested with conventional validation assays. Immunostaining of iChM5Ap23 and iChM5Bp28 cultures showed expression of Oct4 (Fig. 3A), Sox2 and Nanog (see below) that was indistinguishable from expression in H9p45 hESCs. We noted that the variability in Oct4 expression that was detected in newly established populations (Fig. 1) was lost with continued culture, consistent with loss of transgene expression and/or up regulation of endogenous Oct4 expression to equivalent levels. Immunostaining showed expression of the Tra-1-81 and SSEA-5 (Tang et al. 2011) cell surface antigens (Fig. 3A) that are widely used as markers for pluripotency. The developmental potential of iChM5 derivatives was tested with teratoma assays; injection of iChM5Ap14, iChM5Bp14 and control H9p66 hESCs in immunocompromised mice generated teratomas within 9 weeks. Histochemical stains of cryosections showed tissue derivatives of ectoderm, mesoderm and endoderm in tumors derived from iChM5 derivatives and H9 hESC (Fig. 3B), indicating that both iChM5A and iChM5B derivatives have pluripotent developmental potential. High resolution G-banded karyotype analysis of iChM5 derivatives showed a normal 46, XX karyotype at early passages, iChM5Ap14 and iChM5Bp14, as well as late passages, iChM5Ap60 and iChM5Bp60 (Fig. 3C). Prolonged culture of karyotypically normal iChM5 derivatives indicated that iChM5 derivatives were self renewing, in contrast to ChM5 parental cells that senesce near passage 20. These findings collectively indicate that iChM5A and iCh5MB lines are self-renewing, pluripotent and karyotypically normal iPSCs.

Given that rosette assembly was used as preliminary evidence for pluripotency of iChM5 candidates, we next asked whether loss of pluripotency could be directly associated with spontaneous rosette assembly in validated iChM5 derivatives. Immunofluorescence analysis indicated that the bulk of cells (>90%) in iChM5A and iChM5B cultures ($n \geq 3$ of each) expressed Nanog and Sox2 as well as Oct4. Dual labeling showed that nuclear localized Nanog was correlated with nuclear localized Oct4 (Fig. 3D). The absence of nuclear localized Oct4 and Nanog correlated with clusters of more closely apposed cells that were reminiscent of forming neural rosettes. Immunostaining showed all of the cells tested ($n > 500$), with and without colocalized Oct4 and Nanog expression, expressed Sox2 (Fig. 3D and Supplementary Fig. 4), consistent with the known maintenance of Sox2 expression during neural differentiation of PSCs. Dual labeling of Sox2 and Eg5, a well characterized kinesin that binds to cytoplasmic microtubules (Cross & McAinsh 2014), revealed cytoplasmic extensions that suggested changes in cell morphology during early stages of rosette assembly (Fig. 3D). Screens of more than 3

fields of view in at least 3 samples of iChM5A and iChM5B and H9 cells failed to show rosette structures with nuclear localized Oct4 and Nanog. We noted small dots of Nanog immunoreactive signal in a perinuclear position in cells with and without nuclear localized Nanog (Fig. 3D). Given similar localization in HEK293 cells (Supplementary Fig. 4), the signal likely reflects immunoreactivity of a shared or cross reactive epitope that is associated with centrosomes. These collective observations correlate coordinate loss of nuclear localized Oct4 and Nanog, but not Sox2, with the early stages of rosette assembly and validate use of rosette assembly as a sentinel for pluripotency of precursor PSCs.

Molecular analysis of iChM5 derivatives

Episomal vectors are lost when the vector encoded EBNA-1 gene is epigenetically silenced in PSCs and replication of episomes is blocked (Frappier 2012; Yates et al. 1985). Loss of episomes from iChM5 derivatives was evaluated with polymerase chain reaction (PCR), using transgene-specific primers (Supplementary Table 2) to probe genomic DNA of iChM5A and iChM5B derivatives at very early (p4-6), mid (p24-25) and late (p59-60) passages and from parental ChM5p10 cells and MEFs. The EBNA-1 and OriP transgenes were detected in early, but not in later passages of candidate iChM5A and iChM5B lines (Fig. 4A), showing loss of episomes during expansion of candidate lines. Detection of EBNA-1 and OriP was correlated with detection of vector transgenes in early passage iChM5p6 cultures, but not in iChM5Ap34 cultures (Fig. 4B). PCR analysis of genomic DNA and transcript analysis of 4 clonal lines derived from iChM5Ap15 indicated that episomes were lost early during culture expansion (data not shown). These finding show recovery of vector-free iChM5 derivatives.

Demethylation of cytosines in CpG islands in the promoter of Oct4 is essential for conversion of somatic cells into self-renewing iPSCs (Watanabe et al. 2013). Methylation of CpG islands was assayed by bisulfite sequencing of genomic DNA from iChM5Ap18, H9p50 and parental ChM5p10 cells (Freberg et al. 2007). DNA sequence analysis of cloned amplification products (Fig. 4C) showed that CpG motifs between the distal and proximal enhancers in H9p50 (9%, 4.0%) and iChM5Ap18 cells (0%, 2%), respectively, were hypomethylated relative to parental ChM5p10 cells (43%, 31%). The segment between the proximal enhancer and the transcriptional start site showed methylation in both H9p50 and iChM5Ap18 cells (50%, 62%), respectively, that was similar to parental ChM5p10 cells (75%). These observations indicated that genetic

reprogramming induced epigenetic changes in iChM5A derivatives that closely aligned with H9 hESCs. One inference of these findings is that epigenetic silencing underlies the lack of Oct4 expression in parental ChM5 cells and that immunodetection of Oct4 in iChM5A and iChM5B lines reflects epigenetic modifications that allow transcription of Oct4.

Transcription of Oct4 and other genes in the pluripotency network was tested by syber green-based quantitative amplification of cDNA (Fig. 4D). Transcripts of Oct4, Sox2, Nanog and Lin28 were not detected above internal controls in cDNA from parental ChM5 cells, but were detected in iChM5A and iChM5B cells and in H9 hESCs. Transcripts of cMyc were above internal controls in parental ChM5 cells and were similar to levels in iChM5 derivatives and control hESCs although trending lower. Transcript levels in iChM5 derivative NSPs were similar, but up regulation of Sox2 was less dramatic (data not shown). Variation in transcript levels was expected given the potential for differentiation within populations, but Sox2 levels were unexpectedly low. Transcript analysis of immortalized NSPs derived from human fetal ventral midbrain showed down regulation Oct4 and Nanog, but up regulation of Sox2, indicating that the low Sox2 levels in iChM5 candidates and H9 hESCs did not reflect our Sox2 primers, but the relative levels of pluripotency factors in these PSC cultures. Taken together, these results show transcriptional activation of the pluripotency network in iChM5 derivatives.

Somatic cell identity is lost or down regulated during genetic reprogramming. The somatic source(s) of the parental ChM5 mixed cell pool is unknown and cannot be tested a such, but amniotic stromal and epithelial cells alike show stromal cell traits (Wilson et al. 2012). Stromal cell traits of amniotic epithelial cells can reflect epithelial-mesenchymal transition (EMT) in which epithelial cells acquire stromal cell traits by down regulation of E-Cadherin and up regulation of N-Cadherin (Nieto 2011). TaqMan assays were used to probe transcript levels of these cadherins and the EMT inducer TGFβ in cDNA from parental ChM5 cells, iChM5 derivatives, H9 hESCs and BMMSCs as a stromal cell control (Fig. 4E). Transcript analysis showed 10 fold lower levels of N-Cadherin and TGFβ and increased levels of E-Cadherin in iChM5 derivatives in comparison to parental ChM5 cells although slightly lower than levels in H9 hESCs. These findings show loss of stromal cell characteristics by genetic reprogramming of parental ChM5 cells.

Discussion

The overarching goal of this work was to test the feasibility of reprogramming amniotic cells with nonintegrating episomal vectors. We were faced with the common challenge of selecting optimal candidates while conserving limited resources. We report a novel use of neural rosettes as a sentinel for induced pluripotency in candidate iPSC lines and maintenance of pluripotency in validated PSC lines. Spontaneous self-assembly of neural rosettes is unique to PSCs and rosette structures in teratomas are commonly cited as evidence of neural differentiation potential of PSCs. Neural rosettes represent a 3-deminisional primitive tissue that approximates the primordial neural tube in vivo (Elkabetz & Studer 2008; Wilson & Stice 2006). Derivation of neural rosettes has been used primarily to generate cultures of NSPs from PSCs (Ebert et al. 2013; Shin et al. 2006; Yan et al. 2013) or to study signaling pathways in specification of neural subtypes (Chambers et al. 2009), but use of rosette assembly has not been reported in the literature as means to screen and select candidates for expansion and validation.

Self-assembly of neural rosettes as a sentinel for induced pluripotency

Progression through a rosette stage is not essential for directed transdifferentiation of somatic cells into neural derivatives (Ladewig et al. 2013), but self-assembly of neural rosettes is arguably an essential capacity of PSCs and provides a measure of confidence in candidate selection. Rosette assembly has practical value in candidate selection for several reasons. First, rosette assembly can occur by spontaneous differentiation of candidates without application of neural induction protocols. Second, the 3-deminisional structure and organization of rosettes can be readily identified in living cultures by phase imaging and distinguished of from aging MEFs, parental cells and amorphous cell aggregates. Third, spontaneous differentiation of rosettes generates a diverse array of derivative cell types that can be validated by immunostaining of nuclear localized transcription factors (Elkabetz & Studer 2008; Wilson & Stice 2006) and use of dual labeling of different transcription factors to enhance the rigor of the assay. This is a key advantage because nuclear localized transcription factors are superior indicators of neural identity in comparison to more widely used cytoplasmic markers such as nestin and βIII-tubulin that in our hands are sensitive technical artifacts in fixation and immunostaining. Finally, functional tests are less likely to give false positives in comparison to marker expression alone. Expression of pluripotency markers does not guarantee pluripotency; established hESC lines harboring chromosomal abnormalities can express pluripotency factors, but fail to differentiate (Wilson et

al. 2007) and integrated transgenes may not be fully silenced (Malik & Rao 2013; Mostoslavsky 2012; Rao & Malik 2012) and mistaken for expression of endogenous genes.

Rosette assembly distinguished iChM5 candidates from iChM5RCB1 candidates. Neural rosettes formed in backup cultures of iChM5A and iChM5B candidates that were comparable to rosettes in H9 controls (Fig. 2, Supplementary Fig. 2 and Supplementary Fig. 3). Rosettes were not detected in backup cultures of iChMRCB1-derived candidates although these candidates were generated by transfection with the same 3 vector combination that produced iChM5B candidates. Similar results were obtained by transfection of the ChM1 population (data not shown) that is highly enriched for epithelial cells (Wilson et al. 2012). The simplest interpretation of these findings is that amniotic stromal cells are easier to reprogram with episomal vectors than epithelial cells and that differences in reprogramming efficiency is reflected in the differential capacity of the candidates to assemble neural rosettes. Vector systems and reprogramming protocols have improved since we initiated this work and further work could show whether the differences in reprogramming reflect reprogramming methods or differences between epithelial and stromal cell types in amniotic fluid and potentially other sources.

Activation and inactivation of the pluripotency network in iChM5A and iChM5B lines

The value of neural rosettes in candidate selection was substantiated by subsequent validation of pluripotency of iChM5 derivatives, including evidence for epigenetic modification of chromatin structure (Fig. 4C) that activated the endogenous pluripotency network of genes (Fig. 3A, Fig. 3D, Fig. 4D) and transformed ChM5 stromal cells into self-renewing iPSCs with epiblast characteristics (Fig. 4E). Pluripotency is a dynamic state that is difficult to convey in static images, but evidence is critical to discerning differences between expression of pluripotency genes and pluripotent differentiation potential. Here, the dynamic state of pluripotency was evident in spontaneous assembly of neural rosettes in cultures of validated self-renewing iChM5 derivatives; loss of nuclear localized Oct4 and Nanog correlated with changes in cell morphology in forming neural rosettes (Fig. 3D). This immunofluorescence assay is valuable because it is simple, highly reproducible ($n \geq 6$) and can provide critical internal controls in the same culture and within the same field of view. Immunostaining in this case is superior to flow cytometry that cannot discriminate between nuclear and cytoplasmic localization of transcription factors or easily correlate gene expression and changes in cell morphology in differentiating cells.

Teratoma formation is the accepted standard for pluripotent developmental potential and an assay for the safety of iPSC derivatives in clinical applications (Muller et al. 2010). iChM5A and iChM5B derivatives generated teratomas, under the same conditions and within the same timeframe as control H9 hESCs (Fig. 3B). We used VPA during reprogramming of ChM5 cells; VPA is a small molecule inhibitor of histone deacetyltransferases (HDACs) that is widely used in combination with reprogramming factors in the form of transgenes, mRNA or protein to promote reprogramming (Huangfu et al. 2008). Subsets of amniotic cells that were selected for expression of the cKit cell surface receptor, cultured in conditions for hESCs and transiently exposed to VPA showed characteristics of pluripotency, including tumor formation in vivo (Moschidou et al. 2012). We ascribe induced pluripotency of iChM5 derivatives to genetic reprogramming rather than chemical induction by VPA because newly isolated candidates contained episomal vector sequences (Fig. 4) and because VPA produces global effects on transcription levels that are not known to be heritable. The value of teratomas as assays for pluripotency is under discussion (Buta et al. 2013), in part because evaluation of teratoma composition has a subjective component and standards for assigning tissue derivatives could vary among research groups. We favor use of reliable organoid assays in vitro, such as neural rosettes, to characterize differentiation into the 3 germ layer lineages because such assay and their interpretation is more transparent to researchers and because of the availability of rigorous internal controls.

Conclusions and repository access

We show recovery of fully vector-free validated iPSCs by genetic reprogramming of amniotic cells with episomal vectors. Neural rosettes formed by spontaneous assembly provides a sentinel for candidate selection in advance of validation. Coordinated loss of nuclear localized Oct4 and Nanog in emerging neural rosettes in cultures of self-renewing iPSCs provides a simple and reliable assay for a dynamic state of pluripotency to differentiate pluripotent developmental potential of PSCs from expression of pluripotency genes in somatic cells. Rosette assembly and differentiation is not new to stem cell research, but could maximize resource allocation in derivation and use of PSCs and improve the quality and quantity of iPSCs from diverse sources for clinical applications.

The iChM5A and iChM5B lines generated in this work are available as PGW1i:ChM5A and PGW2i:ChM5B on request as resources allow and from the Rutgers University Cell and DNA Repository, 145 Bevier Road Piscataway NJ 08854-8009.

Figure Legends

Main Text

Figure 1. Characterization of parental cells and candidate colonies. Phase images compare the morphology of control H9p54 hESCs with parental ChM5 and ChMRCB1 cells. Inserts are magnified 3X. Note change in size due to higher area of cytoplasm in somatic cells. Magnification is identical within columns. Immunostaining of H9p45 hESCs and candidate iChM5Ap3 and iChMRCB1Ap7 colonies for Oct4 (red) and a fluorescent DNA (blue) dye. Scale bar, 100 microns.

Figure 2. Neural differentiation potential of candidate iChM5 lines. Phase image of H9 and iChM5 derivatives showing rosettes (arrows) in living cultures with insets at 3X magnification. Scale bar, 100 microns in phase images. Rosettes (Rst) and rosette derived NSP populations from H9p47 and iChM5B cultures were immunostained for neural markers as shown. Chromatin in all panels was stained with a fluorescent dye (blue). Inset in rosette collection from H9p47 cells shows a gray scale image of immunostaining for βIII-tubulin alone to better show the density of immature neurons. Scale bars, in microns.

Figure 3. Validation of pluripotency. (A) *Immunostaining of pluripotency markers.* Control H9p45 hESCs, iChM5Ap23 and iChM5Bp28 cells immunostained as indicated. Note uniform Oct4 signal in iChM5 derivatives in comparison to early passages (Fig. 1). Scale bar, 100 microns. (B) *Histochemical stains of teratomas.* Germ layer derivatives of endoderm (endo), ectoderm (ecto) and mesoderm (meso) in columns with examples from each teratoma indicated by asterisks (*). Tissue derivatives were identified with the generous help of Dr. Mark Willingham, a pathologist at Wake Forest University Health Sciences. Magnification is identical in all panels. (C) *Karyotype analysis.* High resolution G-banded karyotype analysis of iChM5A and iChM5B cells at early (p14) and late (p60) passages were analyzed by the Cytogenetics Laboratory of the University of Wisconsin-Madison. (D) *Spontaneous assembly of rosettes in iChM5 derivatives.* Feeder free cultures iChM5Ap15 and iChM5Bp28 cells in chamber slides were immunostained as indicated. Left panel, emerging rosettes among self-renewing iPSCs; grayscale inset shows 1x magnification of immunostaining of Oct4 alone. Middle panel shows Nanog staining alone with inset at 2X magnification showing presumptive centrosomes (arrows).

Right panel shows forming rosettes immunopositive for Sox2 and Eg5. Asterisks (*) in each panel indicates example of forming rosette. Scale bar, 50 microns. Immunostaining of Sox2 in this iChM5Ap15 culture is shown in Supplementary Fig. 4.

Figure 4. Molecular analysis of iChM5A and iChM5B lines. (A) *Amplification of vector sequences.* Genomic DNA probed for vector transgenes (tg) OriP and EBNA-1 and for endogenous (e) GAPDH and Oct4 genes. Note that the eOct4 band is near the gel edge. (B) *Amplification of transgenes*. Genomic DNA from iChM5Ap34 and iChM5Ap6 cells probed for vector transgenes Oct4, Nanog, SV40 T-antigen, Sox2, Lin28, Klf4 and the endogenous copy of Oct4. Range of ladder markers indicated. (C). *Bisulfite sequence analysis*. Oct4 promoter containing a distal enhancer (DE), proximal enhancer (PE), proximal promoter element (PP) and transcription start site (TSS +1). Open and closed circles represent unmethylated and methylated cytosines, respectively, in single clones at the positions indicated. The percentage of methylated cytosines in each clone set is indicated. (D) *Transcript profiles of pluripotency factors*. ΔΔCt values for ChM5p10, H9p44, iChM5Ap18, iChM5Bp20 cells and immortalized human ventral midbrain neural progenitors (hVMNSPs) were normalized to levels of β-glucuronidase (GUSB). cMyc levels in single experiment indicated with asterisks (*) or not determined (n.d.). (E) *Transcript profiles of EMT-associated genes.* ΔΔCt values for H9p44, iChM5Ap15, iChM5Bp37, ChM5Ap10, BMMSCp5 were probed for GUSB, E-Cadherin (ECAD), N-Cadherin (NCAD) and TGFβ with TaqMan gene expression assays and presented as fold expression as normalized to GUSB.

Supplementary Material

Supplementary Figure 1. Vector validation. (A) *PCR analysis*. Amplification of the vector-borne Oct4 transgene (tgOct4) and endogenous chromosomal Oct4 (eOct4) in nontransfected control HEK293 cells (0) and HEK293 cells transfected with 2-vector combination of the pEP4 E02S CK2M EN2L and pEP4 E02S ET2K plasmids at passages 1 through 5 in serum containing media as indicated. Transfected populations were serially passaged, counted with a haemocytomer at each passage and a portion of each population at each passage was used for DNA isolation, immunostaining and seeding new cultures with defined cell numbers. (B) *Immunostaining of Oct4*. The first (HEK293:tf+1) and last passage (HEK293:tf+5) of transfected

cells showed 5% and 0.5%, respectively, of the cells were immunopositive for Oct4. These findings suggested that episomes were not efficiently replicated and were rapidly lost during population expansion in DMEM15% media.

Supplementary Figure 2. Immunofluorescence of rosettes and NSP derivatives. (A). *Rosettes*. Low magnification image of H9 and iChM5 derived rosettes immunostained as indicated. (B) *iChM5Ap4-derived rosettes and NSPs*. Dissociated rosettes from candidate colonies were immunostained as indicated. Rosette immunostained for nestin is indicated by asterisk (*). (A,B) Scale bar, in microns as indicated.

Supplementary Figure 3. Differentiating NSPs. Phase images of NSPB6p12 showing early stage differentiation by withdrawal of mitogens in confluent culture in top image. Middle and bottom images show induced differentiation of NSPB6p12 cells and control hVMNSPs, respectively, at day 7. Representative of presumptive axonal extensions are indicated by arrows. Scale bar, in microns as indicated.

Supplementary Figure 4. Immunostaining of iChM5Ap15 cells and transfected HEK293 cells. Left panel shows immunostaining of Sox2 in the iChM5Ap15 cultures that are shown in Fig. 3D in the main text. Grayscale insert at 2X magnification shows Sox2 expression in presumptive forming rosette (asterisk), identified by the radial arrangement of cells. Right panel shows HEK293 cells transfected with 2-vector combination of pEP4 E02S CK2M EN2L and pEP4 E02S ET2K plasmids. Grayscale inset at 2X magnification shows Nanog signal at presumptive centrosomes (arrow) that are in the same focal plane. Centrosomes that are out of the focal plane are not visible here. Differential staining for Oct4 (red), Nanog (green) or Oct4 and Nanog (yellow) expression reflects the presence of Oct4 on both vectors and Nanog on one vector. Scale bar, 50 microns.

584 **Acknowledgements**

585 We are grateful Cynthia Zimmerman and Laddie Crisp for technical support. The authors
586 received funding support from the Christopher L. Mosley Foundation (PGW), Telemedicine &
587 Advanced Technology Research Center (W81XWH0710718) and the State of North Carolina
588 (G20431003411MED). The funding sources had no involvement in study design; collection,
589 analysis, and interpretation of data or writing and submission of manuscript for publication.

Literature Cited

Anchan RM, Quaas P, Gerami-Naini B, Bartake H, Griffin A, Zhou Y, Day D, Eaton JL, George LL, Naber C, Turbe-Doan A, Park PJ, Hornstein MD, and Maas RL. 2011. Amniocytes can serve a dual function as a source of iPS cells and feeder layers. *Hum Mol Genet* 20:962-974.

Beers J, Gulbranson DR, George N, Siniscalchi LI, Jones J, Thomson JA, and Chen G. 2012. Passaging and colony expansion of human pluripotent stem cells by enzyme-free dissociation in chemically defined culture conditions. *Nat Protoc* 7:2029-2040.

Brace RA. 1997. Physiology of amniotic fluid volume regulation. *Clin Obstet Gynecol* 40:280-289.

Buta C, David R, Dressel R, Emgard M, Fuchs C, Gross U, Healy L, Hescheler J, Kolar R, Martin U, Mikkers H, Muller FJ, Schneider RK, Seiler AE, Spielmann H, and Weitzer G. 2013. Reconsidering pluripotency tests: do we still need teratoma assays? *Stem Cell Res* 11:552-562.

Chambers SM, Fasano CA, Papapetrou EP, Tomishima M, Sadelain M, and Studer L. 2009. Highly efficient neural conversion of human ES and iPS cells by dual inhibition of SMAD signaling. *Nat Biotechnol* 27:275-280.

Cohen M, Briscoe J, and Blassberg R. 2013. Morphogen interpretation: the transcriptional logic of neural tube patterning. *Curr Opin Genet Dev* 23:423-428.

Cross RA, and McAinsh A. 2014. Prime movers: the mechanochemistry of mitotic kinesins. *Nat Rev Mol Cell Biol* 15:257-271.

Dobreva MP, Pereira PN, Deprest J, and Zwijsen A. 2010. On the origin of amniotic stem cells: of mice and men. *Int J Dev Biol* 54:761-777.

Ebert AD, Shelley BC, Hurley AM, Onorati M, Castiglioni V, Patitucci TN, Svendsen SP, Mattis VB, McGivern JV, Schwab AJ, Sareen D, Kim HW, Cattaneo E, and Svendsen CN. 2013. EZ spheres: A stable and expandable culture system for the generation of pre-rosette multipotent stem cells from human ESCs and iPSCs. *Stem Cell Res* 10:417-427.

Elkabetz Y, Panagiotakos G, Al Shamy G, Socci ND, Tabar V, and Studer L. 2008. Human ES cell-derived neural rosettes reveal a functionally distinct early neural stem cell stage. *Genes Dev* 22:152-165.

Elkabetz Y, and Studer L. 2008. Human ESC-derived neural rosettes and neural stem cell progression. *Cold Spring Harb Symp Quant Biol* 73:377-387.

Fan Y, Luo Y, Chen X, Li Q, and Sun X. 2012. Generation of human beta-thalassemia induced pluripotent stem cells from amniotic fluid cells using a single excisable lentiviral stem cell cassette. *J Reprod Dev* 58:404-409.

Ferguson-Smith MA. 2008. Cytogenetics and the evolution of medical genetics. *Genet Med* 10:553-559.

Frappier L. 2012. EBNA1 and host factors in Epstein-Barr virus latent DNA replication. *Curr Opin Virol* 2:733-739.

Freberg CT, Dahl JA, Timoskainen S, and Collas P. 2007. Epigenetic reprogramming of OCT4 and NANOG regulatory regions by embryonal carcinoma cell extract. *Mol Biol Cell* 18:1543-1553.

Galende E, Karakikes I, Edelmann L, Desnick RJ, Kerenyi T, Khoueiry G, Lafferty J, McGinn JT, Brodman M, Fuster V, Hajjar RJ, and Polgar K. 2010. Amniotic fluid cells are more efficiently reprogrammed to pluripotency than adult cells. *Cell Reprogram* 12:117-125.

Ge X, Wang IN, Toma I, Sebastiano V, Liu J, Butte MJ, Reijo Pera RA, and Yang PC. 2012. Human amniotic mesenchymal stem cell-derived induced pluripotent

641 stem cells may generate a universal source of cardiac cells. *Stem Cells Dev*
642 21:2798-2808.
643 Hitoshi S, Seaberg RM, Koscik C, Alexson T, Kusunoki S, Kanazawa I, Tsuji S, and van
644 der Kooy D. 2004. Primitive neural stem cells from the mammalian epiblast
645 differentiate to definitive neural stem cells under the control of Notch
646 signaling. *Genes Dev* 18:1806-1811.
647 Huangfu D, Maehr R, Guo W, Eijkelenboom A, Snitow M, Chen AE, and Melton DA.
648 2008. Induction of pluripotent stem cells by defined factors is greatly
649 improved by small-molecule compounds. *Nat Biotechnol* 26:795-797.
650 Jezierski A, Gruslin A, Tremblay R, Ly D, Smith C, Turksen K, Sikorska M, and Bani-
651 Yaghoub M. 2010. Probing stemness and neural commitment in human
652 amniotic fluid cells. *Stem Cell Rev* 6:199-214.
653 Jiang G, Di Bernardo J, Maiden MM, Villa-Diaz LG, Mabrouk OS, Krebsbach PH, O'Shea
654 KS, and Kunisaki SM. 2014. Human transgene-free amniotic fluid-derived
655 induced pluripotent stem cells for autologous cell therapy. *Stem Cells Dev*.
656 Ladewig J, Koch P, and Brustle O. 2013. Leveling Waddington: the emergence of
657 direct programming and the loss of cell fate hierarchies. *Nat Rev Mol Cell Biol*
658 14:225-236.
659 Li C, Zhou J, Shi G, Ma Y, Yang Y, Gu J, Yu H, Jin S, Wei Z, Chen F, and Jin Y. 2009.
660 Pluripotency can be rapidly and efficiently induced in human amniotic fluid-
661 derived cells. *Hum Mol Genet* 18:4340-4349.
662 Li Q, Fan Y, Sun X, and Yu Y. 2012. Generation of Induced Pluripotent Stem Cells from
663 Human Amniotic Fluid Cells by Reprogramming with Two Factors in Feeder-free
664 Conditions. *J Reprod Dev*.
665 Liu H, and Zhang SC. 2011. Specification of neuronal and glial subtypes from human
666 pluripotent stem cells. *Cell Mol Life Sci* 68:3995-4008.
667 Liu T, Zou G, Gao Y, Zhao X, Wang H, Huang Q, Jiang L, Guo L, and Cheng W. 2012.
668 High Efficiency of Reprogramming CD34(+) Cells Derived from Human
669 Amniotic Fluid into Induced Pluripotent Stem Cells with Oct4. *Stem Cells Dev*
670 21:2322-2332.
671 Lu HE, Tsai MS, Yang YC, Yuan CC, Wang TH, Lin XZ, Tseng CP, and Hwang SM. 2011.
672 Selection of alkaline phosphatase-positive induced pluripotent stem cells from
673 human amniotic fluid-derived cells by feeder-free system. *Exp Cell Res*
674 317:1895-1903.
675 Maguire CT, Demarest BL, Hill JT, Palmer JD, Brothman AR, Yost HJ, and Condic ML.
676 2013. Genome-wide analysis reveals the unique stem cell identity of human
677 amniocytes. *PLoS One* 8:e53372.
678 Malchenko S, Xie J, de Fatima Bonaldo M, Vanin EF, Bhattacharyya BJ, Belmadani A,
679 Xi G, Galat V, Goossens W, Seftor RE, Tomita T, Crispino J, Miller RJ, Bohn MC,
680 Hendrix MJ, and Soares MB. 2014. Onset of rosette formation during
681 spontaneous neural differentiation of hESC and hiPSC colonies. *Gene* 534:400-
682 407.
683 Malik N, and Rao MS. 2013. A review of the methods for human iPSC derivation.
684 *Methods Mol Biol* 997:23-33.
685 Moschidou D, Mukherjee S, Blundell MP, Jones GN, Atala AJ, Thrasher AJ, Fisk NM, De
686 Coppi P, and Guillot PV. 2012. Human Mid-Trimester Amniotic Fluid Stem Cells
687 Cultured Under Embryonic Stem Cell Conditions with Valproic Acid Acquire
688 Pluripotent Characteristics. *Stem Cells Dev*.
689 Mostoslavsky G. 2012. Concise review: The magic act of generating induced
690 pluripotent stem cells: many rabbits in the hat. *Stem Cells* 30:28-32.
691 Muller FJ, Goldmann J, Loser P, and Loring JF. 2010. A call to standardize teratoma
692 assays used to define human pluripotent cell lines. *Cell Stem Cell* 6:412-414.

693 Murphy SV, and Atala A. 2013. Amniotic fluid and placental membranes: unexpected
694 sources of highly multipotent cells. *Semin Reprod Med* 31:62-68.
695 Nieto MA. 2011. The ins and outs of the epithelial to mesenchymal transition in
696 health and disease. *Annu Rev Cell Dev Biol* 27:347-376.
697 Rao MS, and Malik N. 2012. Assessing iPSC reprogramming methods for their
698 suitability in translational medicine. *J Cell Biochem* 113:3061-3068.
699 Robinton DA, and Daley GQ. 2012. The promise of induced pluripotent stem cells in
700 research and therapy. *Nature* 481:295-305.
701 Shin S, Mitalipova M, Noggle S, Tibbitts D, Venable A, Rao R, and Stice SL. 2006.
702 Long-term proliferation of human embryonic stem cell-derived neuroepithelial
703 cells using defined adherent culture conditions. *Stem Cells* 24:125-138.
704 Takahashi K, Okita K, Nakagawa M, and Yamanaka S. 2007. Induction of pluripotent
705 stem cells from fibroblast cultures. *Nat Protoc* 2:3081-3089.
706 Tang C, Lee AS, Volkmer JP, Sahoo D, Nag D, Mosley AR, Inlay MA, Ardehali R, Chavez
707 SL, Pera RR, Behr B, Wu JC, Weissman IL, and Drukker M. 2011. An antibody
708 against SSEA-5 glycan on human pluripotent stem cells enables removal of
709 teratoma-forming cells. *Nat Biotechnol* 29:829-834.
710 Thomson JA, Itskovitz-Eldor J, Shapiro SS, Waknitz MA, Swiergiel JJ, Marshall VS, and
711 Jones JM. 1998. Embryonic stem cell lines derived from human blastocysts.
712 *Science* 282:1145-1147.
713 Trounson A, Shepard KA, and DeWitt ND. 2012. Human disease modeling with
714 induced pluripotent stem cells. *Curr Opin Genet Dev* 22:509-516.
715 Turner M, Leslie S, Martin NG, Peschanski M, Rao M, Taylor CJ, Trounson A, Turner D,
716 Yamanaka S, and Wilmut I. 2013. Toward the development of a global induced
717 pluripotent stem cell library. *Cell Stem Cell* 13:382-384.
718 Underwood MA, Gilbert WM, and Sherman MP. 2005. Amniotic Fluid: Not Just Fetal
719 Urine Anymore. *J Perinatol* 25:341-348.
720 Watanabe A, Yamada Y, and Yamanaka S. 2013. Epigenetic regulation in pluripotent
721 stem cells: a key to breaking the epigenetic barrier. *Philos Trans R Soc Lond B*
722 *Biol Sci* 368:20120292.
723 Wilson PG, Cherry JJ, Schwamberger S, Adams AM, Zhou J, Shin S, and Stice SL.
724 2007. An SMA project report: neural cell-based assays derived from human
725 embryonic stem cells. *Stem Cells Dev* 16:1027-1041.
726 Wilson PG, Devkota L, Payne T, Crisp L, Winter A, and Wang Z. 2012. Clonal
727 populations of amniotic cells by dilution and direct plating: evidence for
728 hidden diversity. *Stem Cells Int* 2012:485950.
729 Wilson PG, and Stice SS. 2006. Development and differentiation of neural rosettes
730 derived from human embryonic stem cells. *Stem Cell Rev* 2:67-77.
731 Wolfrum K, Wang Y, Prigione A, Sperling K, Lehrach H, and Adjaye J. 2010. The
732 LARGE principle of cellular reprogramming: lost, acquired and retained gene
733 expression in foreskin and amniotic fluid-derived human iPS cells. *PLoS One*
734 5:e13703.
735 Yamanaka S. 2012. Induced pluripotent stem cells: past, present, and future. *Cell*
736 *Stem Cell* 10:678-684.
737 Yan Y, Shin S, Jha BS, Liu Q, Sheng J, Li F, Zhan M, Davis J, Bharti K, Zeng X, Rao M,
738 Malik N, and Vemuri MC. 2013. Efficient and rapid derivation of primitive
739 neural stem cells and generation of brain subtype neurons from human
740 pluripotent stem cells. *Stem Cells Transl Med* 2:862-870.
741 Yates JL, Warren N, and Sugden B. 1985. Stable replication of plasmids derived from
742 Epstein-Barr virus in various mammalian cells. *Nature* 313:812-815.
743 Ye L, Chang JC, Lin C, Qi Z, Yu J, and Kan YW. 2010. Generation of induced pluripotent
744 stem cells using site-specific integration with phage integrase. *Proc Natl Acad*
745 *Sci U S A* 107:19467-19472.

746 Yu J, Hu K, Smuga-Otto K, Tian S, Stewart R, Slukvin, II, and Thomson JA. 2009.
747 Human induced pluripotent stem cells free of vector and transgene
748 sequences. *Science* 324:797-801.
749 Zhang SC. 2006. Neural subtype specification from embryonic stem cells. *Brain*
750 *Pathol* 16:132-142.

Figure 1

Characterization of parental cells and candidate colonies.

Phase images compare the morphology of control H9p54 hESCs with parental ChM5 and ChMRCB1 cells. Inserts are magnified 3X. Note change in size due to higher area of cytoplasm in somatic cells. Magnification is identical within columns. Immunostaining of H9p45 hESCs and candidate iChM5Ap3 and iChMRCB1Ap7 colonies for Oct4 (red) and a fluorescent DNA (blue) dye. Scale bar, 100 microns.

PeerJ PrePrints | http://dx.doi.org/10.7287/peerj.preprints.449v1 | CC-BY 4.0 Open Access | received: 31 Jul 2014, published: 31 Jul

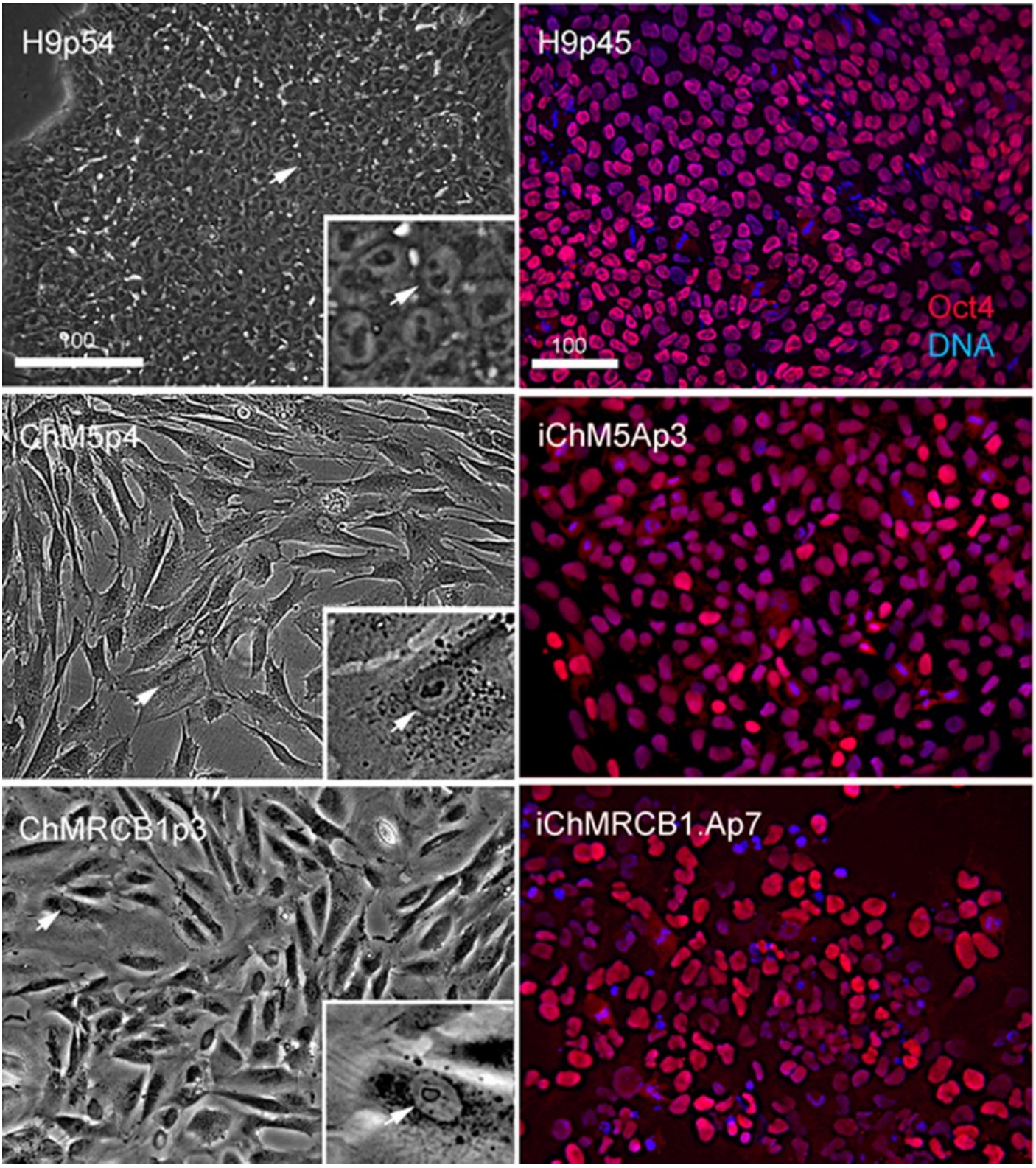

PeerJ PrePrints | http://dx.doi.org/10.7287/peerj.preprints.449v1 | CC-BY 4.0 Open Access | received: 31 Jul 2014, published: 31 Jul

Figure 2

Neural differentiation potential of candidate iChM5 lines.

Phase image of H9 and iChM5 derivatives showing rosettes (arrows) in living cultures with insets at 3X magnification. Scale bar, 100 microns in phase images. Rosettes (Rst) and rosette derived NSP populations from H9p47 and iChM5B cultures were immunostained for neural markers as shown. Chromatin in all panels was stained with a fluorescent dye (blue). Inset in rosette collection from H9p47 cells shows a gray scale image of immunostaining for III-tubulin alone to better show the density of immature neurons. Scale bars, in microns.

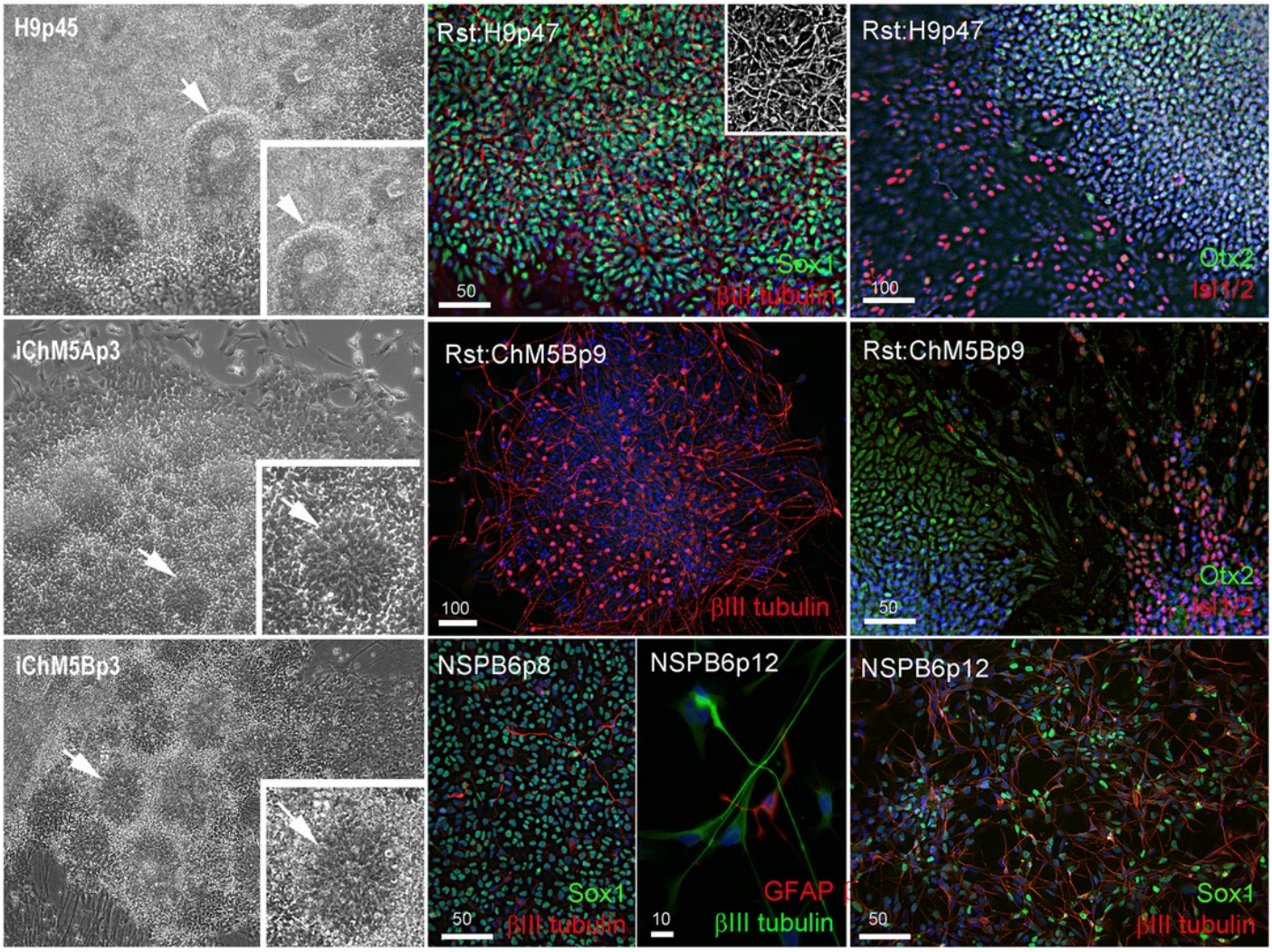

PeerJ PrePrints | http://dx.doi.org/10.7287/peerj.preprints.449v1 | CC-BY 4.0 Open Access | received: 31 Jul 2014, published: 31 Jul

Figure 3

Validation of pluripotency.

PeerJ PrePrints | http://dx.doi.org/10.7287/peerj.preprints.449v1 | CC-BY 4.0 Open Access | received: 31 Jul 2014, published: 31 Jul

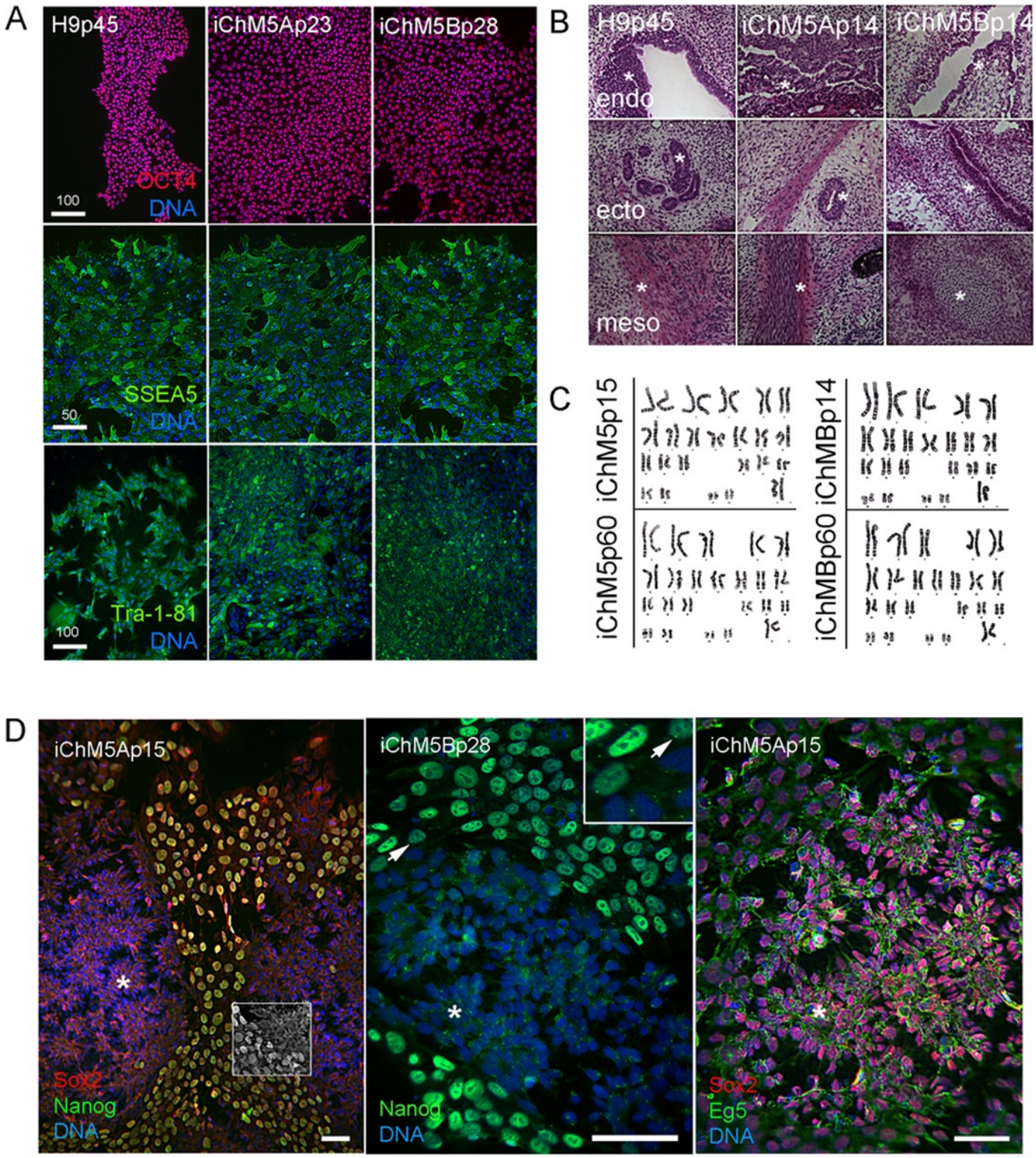

Figure 4

Molecular analysis of iChM5A and iChM5B lines.

(A) ***Amplification of vector sequences.*** Genomic DNA probed for vector transgenes (tg) OriP and EBNA-1 and for endogenous (e) GAPDH and Oct4 genes. Note that the eOct4 band is near the gel edge. (B) *Amplification of transgenes*. Genomic DNA from iChM5Ap34 and iChM5Ap6 cells probed for vector transgenes Oct4, Nanog, SV40 T-antigen, Sox2, Lin28, Klf4 and the endogenous copy of Oct4. Range of ladder markers indicated. (C). *Bisulfite sequence analysis*. Oct4 promoter containing a distal enhancer (DE), proximal enhancer (PE), proximal promoter element (PP) and transcription start site (TSS +1). Open and closed circles represent unmethylated and methylated cytosines, respectively, in single clones at the positions indicated. The percentage of methylated cytosines in each clone set is indicated. (D) *Transcript profiles of pluripotency factors*. DD Ct values for ChM5p10, H9p44, iChM5Ap18, iChM5Bp20 cells and immortalized human ventral midbrain neural progenitors (hVMNSPs) were normalized to levels of b -glucuronidase (GUSB). cMyc levels in single experiment indicated with asterisks (*) or not determined (n.d.). (E) *Transcript profiles of EMT-associated genes.* DD Ct values for H9p44, iChM5Ap15, iChM5Bp37, ChM5Ap10, BMMSCp5 were probed for GUSB, E-Cadherin (ECAD), N-Cadherin (NCAD) and TGF b with TaqMan gene expression assays and presented as fold expression normalized to GUSB.

PeerJ PrePrints | http://dx.doi.org/10.7287/peerj.preprints.449v1 | CC-BY 4.0 Open Access | received: 31 Jul 2014, published: 31 Jul

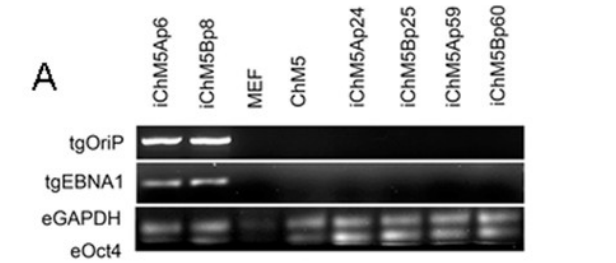

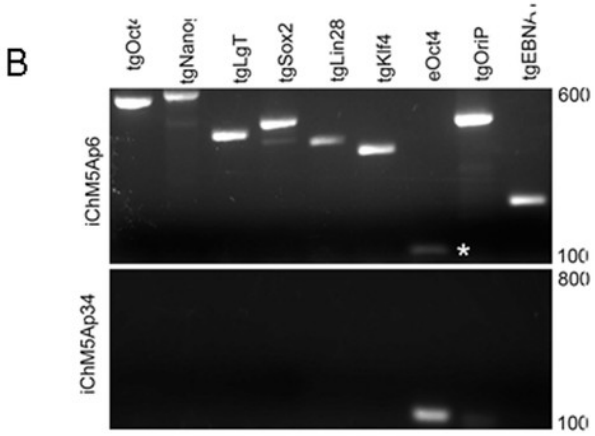

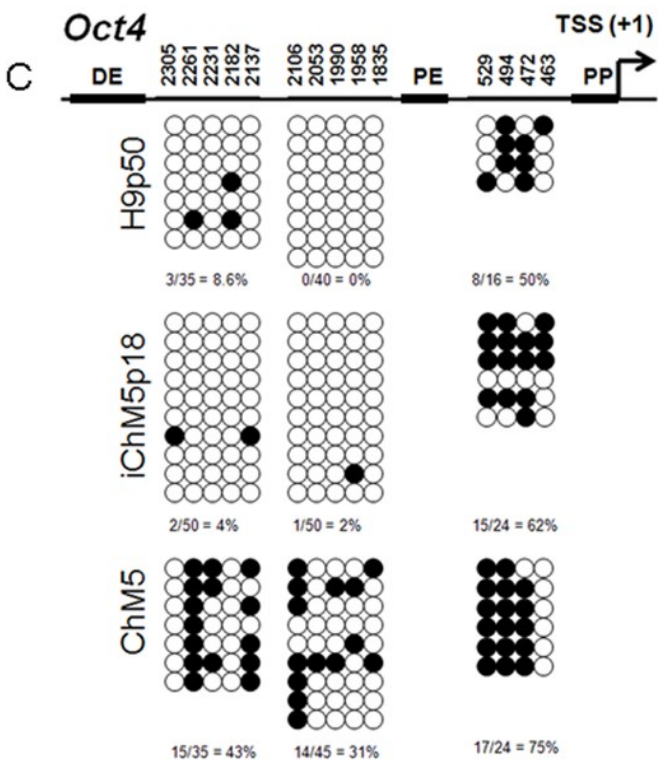

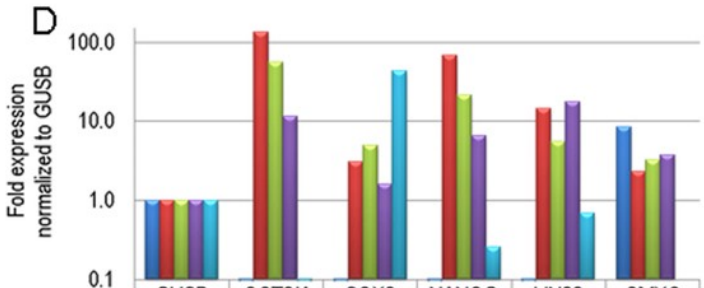

	GUSB	OCT3/4	SOX2	NANOG	LIN28	CMYC
ChM5p10	1.0	0.0	0.0	0.0	0.0	8.3
H9p44	1.0	132.8	3.0	68.9	14.4	2.3
iChM5Ap15	1.0	55.7	5.0	21.4	5.6	3.2*
iChM5Bp25	1.0	11.4	1.6	6.5	17.8	3.8*
VMNPp4	1.0	0.0	43.2	0.3	0.7	n.d.

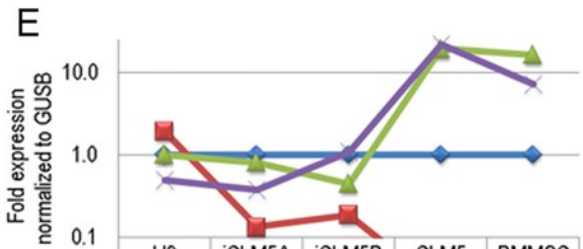

	H9	iChM5A	iChM5B	ChM5	BMMSC
GUSB	1.0	1.0	1.0	1.0	1.0
ECAD	1.9	0.1	0.2	0.0	0.0
NCAD	1.0	0.8	0.4	19.5	16.5
TGFb	0.5	0.4	1.1	22.0	7.3

PeerJ PrePrints | http://dx.doi.org/10.7287/peerj.preprints.449v1 | CC-BY 4.0 Open Access | received: 31 Jul 2014, published: 31 Jul